

## Life Stages: Interactions and Spatial Patterns

Suzanne L. Robertson · J.M. Cushing ·  
R.F. Costantino

Received: 7 June 2011 / Accepted: 4 November 2011 / Published online: 2 December 2011  
© Society for Mathematical Biology 2011

**Abstract** In many stage-structured species, different life stages often occupy separate spatial niches in a heterogeneous environment. Life stages of the giant flour beetle *Tribolium brevicornis* (Leconte), in particular adults and pupae, occupy different locations in a homogeneous habitat. This unique spatial pattern does not occur in the well-studied stored grain pests *T. castaneum* (Herbst) and *T. confusum* (Duval). We propose density dependent dispersal as a causal mechanism for this spatial pattern. We model and explore the spatial dynamics of *T. brevicornis* with a set of four density dependent integrodifference and difference equations. The spatial model exhibits multiple attractors: a spatially uniform attractor and a patchy attractor with pupae and adults spatially separated. The model attractors are consistent with experimental observations.

**Keywords** Spatial distribution · Life stage interactions · Density dependent dispersal · Flour beetle · Integrodifference equations

---

S.L. Robertson (✉)

Interdisciplinary Program in Applied Mathematics, University of Arizona, Tucson, AZ 85721, USA  
e-mail: [srobertson@mbi.osu.edu](mailto:srobertson@mbi.osu.edu)

*Present address:*

S.L. Robertson  
Mathematical Biosciences Institute, The Ohio State University, 1735 Neil Avenue, Columbus,  
OH 43210, USA

J.M. Cushing

Department of Mathematics, University of Arizona, Tucson, AZ 85721, USA

R.F. Costantino

Department of Ecology and Evolutionary Biology, University of Arizona, Tucson, AZ 85721, USA

## 1 Introduction

Spatial segregation of life stages is a common occurrence in stage-structured species. In many circumstances, the spatial separation of life stages occurs in heterogeneous environments, resulting in each stage occupying a separate spatial niche (Jormalainen and Shuster 1997; Ribes et al. 1996; Hill 1988; Hunte and Myers 1984). In cannibalistic species, the physical separation of predator and prey stages can serve to reduce predation mortality. There is evidence of the vulnerable stage moving in response to the cannibalistic stage (Leonardsson 1991), suggesting that the spatial distribution of life cycle stages in certain cannibalistic species may be the result of density dependent avoidance mechanisms.

Density dependent dispersal mechanisms can also be found in aphids. Aphid larvae can develop into one of two adult morphs—winged or wingless. Studies reveal that the proportion of adults having the winged morph (which aids in dispersal of the population) is density dependent, changing with the number of tactile encounters larvae have with other aphids (Harrison 1980). Another example of a density dependent polymorphism affecting dispersal ability is wing length in the brown planthopper *Nilaparvata lugens* (Kisimoto 1956). Nymphs developing under crowded conditions lead to a greater fraction of long-winged adults.

The spatial segregation of pupae and adults in the giant flour beetle *Tribolium brevicornis* in a homogeneous habitat suggests that life stage interactions alone may be sufficient for the formation of nonuniform spatial patterns. While the giant flour beetle is a cannibalistic species, the vulnerable stages are immobile and, therefore, unable to avoid cannibalism directly. Our hypothesis is that the spatial patterns of *T. brevicornis* are the consequence of density dependent dispersal driven by the interactions among the life stages.

We begin by presenting the observed spatial patterns in flour beetle populations that motivated this work. Next, we discuss the unique biological features of the species *T. brevicornis* and write a difference equation model to describe its population dynamics. We then develop a stage structured integrodifference equation model to describe the spatial dynamics and give conditions under which density dependent dispersal can lead to spatial segregation of the life stages.

## 2 Empirical Spatial Patterns

On the surface of a homogeneous container of flour, adults and pupae of the giant flour beetle *T. brevicornis* cluster in separate life stage groups rather than disperse uniformly over the surface of the media (Fig. 1). The segregation of the life stages has not been reported in any of the other 25 species in the genus *Tribolium*. However, there is evidence of spatial segregation in the depth distribution of larvae and adults of *T. castaneum* and *T. confusum* in cylindrical vials of flour (Ghent 1966) that may result from density dependent dispersal (Robertson and Cushing 2011a, 2011b).

Patterns similar to those in Fig. 1, showing the segregation of adults and the other life stages, are seen on the surface of domains of many different shapes and sizes, including rectangular boxes and cylindrical vials. Adults have been observed aggregating along the boundaries of the domains as well as in the interior. The specific

**Fig. 1** Culture of *T. brevicornis* showing segregation of adults (black, in two dense clusters) and pupae (tan colored, primarily on the left side and top) in a 12'' by 9'' box



location of the adults varies greatly among cultures, even among containers of the same size and shape.

### 3 Genus Perspective

There are 26 species of flour beetles in the genus *Tribolium*. *T. castaneum* and *T. confusum* are major pests of stored grain in the world and are the most extensively studied species of the genus. Among the species in the genus there are currently five known types of interactions among the life stages: larvae eat eggs, adults eat eggs, adults eat pupae, adults inhibit larval metamorphosis, and larvae inhibit larval metamorphosis. These interactions appear in different species in different combinations. They do not all appear in any one species. In cultures with two or more species, these interactions form the basis for competition in this genus. The time spent in each life stage also varies among species. In this section, we focus on the species *T. brevicornis*, comparing and contrasting it with *T. castaneum* (we note *T. castaneum* and *T. confusum* share the same stage transitions and interactions).

#### 3.1 Species Comparison

The species *T. brevicornis* and *T. castaneum* have four life stages: egg, larva, pupa, and adult. The larvae and adults of both species eat eggs. However, there are several major biological differences between the species (Sokoloff et al. 1980; Jillson and Costantino 1980). First, *T. brevicornis* adults inhibit larval metamorphosis (Jillson and Costantino 1980) which does not occur in *T. castaneum*. *T. brevicornis* larvae may remain in the larval stage indefinitely until local adult densities lower and they can pupate. Secondly, the innate length of the larval stage for *T. brevicornis* (in the absence of adults) is four weeks, two weeks longer than *T. castaneum*. Larvae are noticeably larger and more mobile in the latter 2-week period than the former. A third notable biological difference between these species is the absence of pupal cannibalism by adults in *T. brevicornis*. Pupal cannibalism is a mechanism that controls adult recruitment in *T. castaneum*; *T. brevicornis* has the alternate control mechanism of inhibition. The life cycles for *T. castaneum* and *T. brevicornis* are shown in Fig. 2.

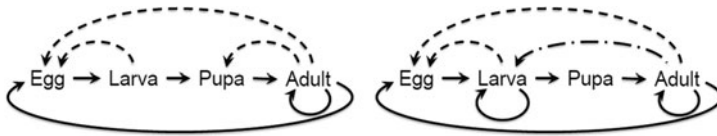


**Fig. 2** Life cycles of *Tribolium castaneum* (left) and *T. brevicornis* (right). Solid arrows indicate transitions between life stages. Dotted lines denote interstage predation; both species exhibit cannibalism of eggs by larvae and adults, and *T. castaneum* adults also cannibalize pupae. The dot-dashed line indicates inhibition; *T. brevicornis* larvae are prevented from pupating in the presence of high adult densities, and can remain in the larval stage until local adult densities are low enough to complete their life cycle

In order to model the spatial dynamics observed in *T. brevicornis*, we first need a nonspatial model to describe the population dynamics of the species. The dynamics of *T. castaneum* are well described by a system of three nonlinear difference equations known as the Larva–Pupa–Adult or LPA model (Cushing 2004; Cushing et al. 2003; Dennis et al. 1995). We note eggs are not modeled, as the length of the egg stage is short relative to the other three stages (Dennis et al. 1995). In the next section, we present the LPA model and then modify it to take into account the biological differences between these species.

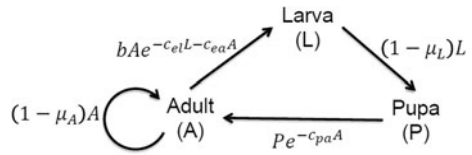
### 3.2 LPA Model of *T. castaneum*

The LPA model is a stage-structured nonlinear difference equation model designed to describe the population dynamics of the flour beetle *T. castaneum* (Cushing 2004):

$$\begin{aligned}
 L_{t+1} &= bA_t \exp(-c_{el}L_t - c_{ea}A_t) \\
 P_{t+1} &= (1 - \mu_L)L_t \\
 A_{t+1} &= P_t \exp(-c_{pa}A_t) + (1 - \mu_A)A_t
 \end{aligned}
 \tag{1}$$

$L_t$ ,  $P_t$ , and  $A_t$  represent the number of individuals in the L-stage (feeding larvae), P-stage (which includes nonfeeding larvae, pupae, and callow adults) and A-stage (sexually mature adults) at time  $t$ , respectively. The time step for the model is 2 weeks, the amount of time spent in the  $L$  and  $P$  stages. Recruitment into the larval class occurs at an inherent rate  $b$ , and eggs must survive cannibalism by larvae and adults in order to become larvae. The term  $\exp(-c_{el}L_t - c_{ea}A_t)$  represents the survival rate of eggs per unit time, where  $c_{el} \geq 0$  and  $c_{ea} \geq 0$  are cannibalism coefficients of eggs by larvae and eggs by adults, respectively. The larval death rate is denoted by  $\mu_L$ ,  $0 < \mu_L < 1$ . The death rate of pupae is negligible, so no  $\mu_P$  term is included in the model. Pupae must escape cannibalism by adults ( $c_{pa}$ ) to emerge as adults at the next time step. Adults die at a rate  $\mu_A$ ,  $0 < \mu_A < 1$ , and so the fraction of adults surviving to the next census is  $(1 - \mu_A)$ . A flow diagram of the LPA model depicting transitions between life stages is given in Fig. 3. We note that while the LPA model was originally developed for *T. castaneum*, it has also been successful at modeling the dynamics of *T. confusum* (Benoit et al. 1998).

**Fig. 3** Flow diagram of the LPA model (1) for *Tribolium castaneum*. The time step between stages is two weeks



### 3.3 SLPA Model of *T. brevicornis*

In this section, we modify the LPA model to incorporate the biology of *T. brevicornis*. In order to account for the longer larval stage, we split the *L* stage of the LPA model into two new stages and denote them by *S* and *L*.  $S_t$  represents the number of younger or “small” larvae at time  $t$  and  $L_t$  now represents the number of “large” larvae at time  $t$ . This class includes third week and fourth week old larvae, as well as older larvae who have failed to pupate due to inhibition. The time step of the model remains 2 weeks. We model inhibition with a Ricker type, or exponential, nonlinearity. This is appropriate given the assumption that inhibition is a result of random tactile encounters of larvae with adults at a rate  $k_i$  and the fraction of larvae inhibited increases with the density of adults. This is the same modeling methodology used to describe cannibalism (Cushing et al. 2003). *T. brevicornis* eggs are subject to cannibalism by small larvae as well as large larvae. Since large larvae have been observed to be more voracious eaters than small larvae, we allow each larval stage its own cannibalism rate (Hastings and Costantino 1991). Thus,  $c_{es}$  is the cannibalism coefficient of eggs by small larvae, and  $c_{el}$  is the cannibalism coefficient of eggs by large larvae. Since adults do not eat pupae the coefficient for this term, which appears in the LPA model, is zero (Jillson and Costantino 1980). Pupal mortality is zero. The SLPA (Small larva–Large larva–Pupa–Adult) model is given by the following equations:

$$\begin{aligned}
 S_{t+1} &= bA_t \exp(-c_{es}S_t - c_{el}L_t - c_{ea}A_t) \\
 L_{t+1} &= S_t + (1 - \mu_L)(1 - \exp(-k_i A_t))L_t \\
 P_{t+1} &= (1 - \mu_L) \exp(-k_i A_t)L_t \\
 A_{t+1} &= P_t + (1 - \mu_A)A_t.
 \end{aligned}
 \tag{2}$$

As in the LPA model,  $P_t$  represents the number of nonfeeding larvae, pupae, and callow adults, and  $A_t$  represents the number of sexually mature adults at time  $t$ . We note that when the inhibition constant  $k_i = 0$ , all surviving large larvae pupate after one time step. If either the inhibition constant or adult density is large, the fraction of large larvae pupating will be small. A flow diagram of the SLPA model depicting transitions between life stages is given in Fig. 4. The SLPA model (2) can also be written in matrix form:

$$\vec{n}_{t+1} = \hat{P}(\vec{n}_t)\vec{n}_t
 \tag{3}$$

where

$$\vec{n}_t = \begin{pmatrix} S_t \\ L_t \\ P_t \\ A_t \end{pmatrix}
 \tag{4}$$

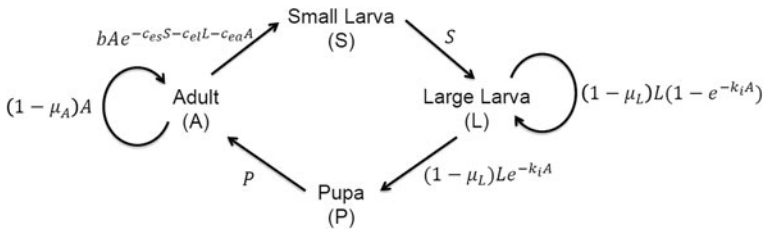


**Fig. 4** Flow diagram of the SLPA model (2) for *Tribolium brevicornis*. The time step between stages is two weeks

**Table 1** Maximum likelihood parameter estimates for the SLPA model. (\* $\mu_A$  calculated from data)

Parameter	Estimate
$b$	11.4096
$c_{es}$	0.0135
$c_{el}$	0.0169
$c_{ea}$	0.0223
$\mu_L$	0.1339
$k_i$	0.0194
* $\mu_A$	0.0158

and

$$\hat{P}(\vec{n}_t) = \begin{bmatrix} 0 & 0 & 0 & b \exp(-c_{es}S_t - c_{el}L_t - c_{ea}A_t) \\ 1 & (1 - \mu_L)(1 - \exp(-k_i A_t)) & 0 & 0 \\ 0 & (1 - \mu_L) \exp(-k_i A_t) & 0 & 0 \\ 0 & 0 & 1 & 1 - \mu_A \end{bmatrix} \tag{5}$$

In order to construct a spatial model for *T. brevicornis*, maximum likelihood parameter estimates were first calculated for the non-spatial SLPA model. Details are given in Robertson (2009), and follow the parameterization methodology outlined in Dennis et al. (1995). The adult death rate,  $\mu_A$ , was not included in the maximum likelihood parameterization but rather calculated directly as  $\mu_A = 0.0158$  based on recorded observations of the number of dead adults at each census. Thus, there are 6 remaining unknown parameters in the deterministic model equations. Maximum likelihood estimates for these parameters are given in Table 1. The deterministic SLPA model with the maximum likelihood parameter estimates in Table 1 predicts an equilibrium. The equilibrium stage vector is  $(S^*, L^*, P^*, A^*) = (12.21, 71.77, 2.59, 163.84)$ . Numerical simulations show that as the inhibition parameter  $k_i$  increases, all other parameters remaining fixed, the number of large larvae in the equilibrium stage vector increases until eventually  $L$  is the dominant stage with  $L^* > A^*$ .

### 4 The Spatial SLPA Model

In this section we construct a spatial extension of the SLPA model on a spatial domain  $\Omega$ , following the modeling methodology for structured populations with density dependent dispersal developed in Robertson (2009). We assume that population dynamics (reproduction and class transitions) occur first each time step, followed by dispersal, using general stage-structured integrodifference equation models that incorporate density dependent dispersal in two ways.

For each stage  $j$ ,  $j \in \{S, L, P, A\}$ , density may affect an individual’s probability of dispersing (determined by a decision function,  $\gamma_j$ ), and/or the probability of moving to another spatial location, given dispersal occurs (determined by a dispersal kernel,  $K_j$ ). In general, these processes may depend on the density of any stage at any spatial location(s), in addition to possible explicit spatial dependence.

These kinds of spatial models have been successfully applied to *T. castaneum* and *T. confusum* (Robertson and Cushing 2011a). Theoretical treatments of equations of this type can be found in Robertson (2009), Robertson and Cushing (2011b).

Not all life-stages of *T. brevicornis* disperse. Pupae are sedentary, so  $\gamma_P \doteq 0$ . Since younger larvae in their first 2 weeks are smaller and slower than older larvae, we make the simplifying assumption that larvae in the *S* class do not disperse ( $\gamma_S \doteq 0$ ). This is consistent with observations of *T. brevicornis* cultures. The remaining two stages, *L* and *A*, are dispersers. We assume adults always disperse ( $\gamma_A \doteq 1$ ) and the fraction of large larvae dispersing depends on the local density of adults.

Although the patterns observed in *T. brevicornis* have all been on a two-dimensional surface, we take advantage of an approximate cross-sectional symmetry in some patterns observed in *T. brevicornis* (namely, those in Figs. 11 and 12, described in Sect. 6) and model one spatial dimension by choosing  $\Omega$  to be a finite interval  $[0, M]$ . We note there were no inherent or observed heterogeneities in the surface habitat, as the incubator where cultures were kept is dark and all locations were under the same temperature and humidity conditions. For modeling dispersal on this domain, we assume no explicit spatial dependence of movement. Rather, we assume that adult beetles tend to prefer locations with lower pupal densities than their starting location. This is biologically reasonable since pupae are more likely to pupate and enter the sexually mature adult class with a lower incidence of tactile contact with adults. Recall that adults do not eat pupae. We incorporate density dependent dispersal into the adult kernel by an exponentially decreasing function of pupal density, recalling pupal density is determined by the density of larvae and adults at the previous time step. Specifically,  $K_A = K_A(\bar{n}_t(x))$  where

$$K_A(\bar{n}_t(x)) \doteq \frac{1}{C} \exp\{-D_{AP}((1 - \mu_L) \exp\{-k_i A_t(x)\} L_t(x))\}. \tag{6}$$

Here,  $C$  is a normalization constant to ensure the integral over space of  $K_A$  is equal to one and  $D_{AP}$  denotes the sensitivity of adults to pupae.

Large larvae do not avoid small larvae or pupae; they do avoid adults. With high adult densities large larvae are inhibited and are unable to pupate; consequently, consistent with the biology we assume that local adult density affects the fraction of large larvae dispersing at any time and location. We model the fraction of large larvae dispersing at each time step by an increasing function of local adult density, making

the simplifying assumption that dispersing large larvae then redistribute uniformly over the entire habitat. These assumptions lead to the following decision function and dispersal kernel for large larvae:

$$\gamma_L(\vec{n}_t(x)) \doteq 1 - \exp\{-D_{LA}(P_t(x) + (1 - \mu_A)A_t(x))\}, \tag{7}$$

$$K_L \doteq \frac{1}{M} \tag{8}$$

where  $D_{LA}$  represents sensitivity of larvae to adults.

Incorporating the dispersal kernels, decision functions, and SLPA population dynamics, we arrive at the following spatial SLPA model written in matrix form—a stage-structured density dependent integrodifference equation model on the homogeneous spatial domain  $\Omega = [0, M]$ :

$$\begin{aligned} \vec{n}_{t+1}(x) = & \int_0^M K(\vec{n}_t(x))\Gamma(\vec{n}_t(y))\hat{P}(\vec{n}_t(y))\vec{n}_t(y)dy \\ & + (I - \Gamma(\vec{n}_t(x)))\hat{P}(\vec{n}_t(x))\vec{n}_t(x) \end{aligned} \tag{9}$$

where  $K(\vec{n}_t(x)) = \text{diag}(0, K_L, 0, K_A(\vec{n}_t(x)))$  with  $K_L$  and  $K_A(\vec{n}_t(x))$  as in (8) and (6),  $\Gamma(\vec{n}_t(x)) = \text{diag}(0, \gamma_L(\vec{n}_t(x)), 0, 1)$  with  $\gamma_L(\vec{n}_t(x))$  as in (7), and  $\hat{P}(\vec{n}_t(x))$  as given by (5). We can also write (9) as the following system of difference and integrodifference equations:

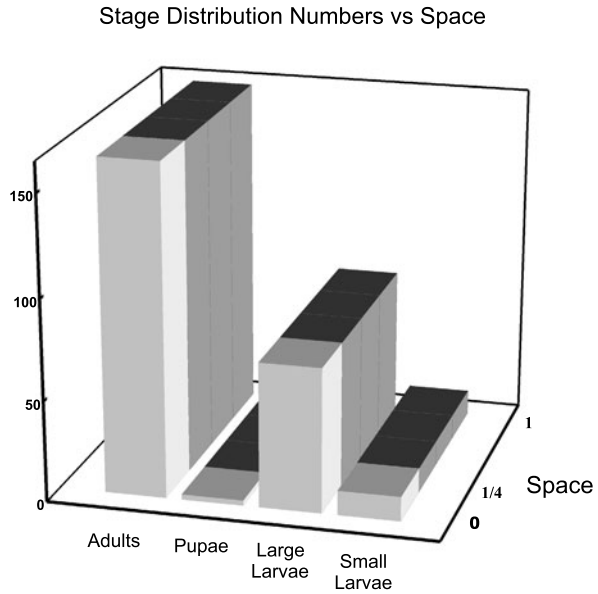
$$\begin{aligned} S_{t+1}(x) &= bA_t(x) \exp\{-c_{es}S_t(x) - c_{el}L_t(x) - c_{ea}A_t(x)\} \\ L_{t+1}(x) &= \int_0^M \frac{1}{M} [1 - \exp\{-D_{LA}(P_t(y) + (1 - \mu_A)A_t(y))\}] \\ &\quad \times [S_t(y) + (1 - \mu_L)(1 - \exp\{-k_iA_t(y)\})L_t(y)] dy \\ &\quad + \exp\{-D_{LA}(P_t(x) + (1 - \mu_A)A_t(x))\} \\ &\quad \times [S_t(x) + (1 - \mu_L)(1 - \exp\{-k_iA_t(x)\})L_t(x)] \\ P_{t+1}(x) &= (1 - \mu_L) \exp\{-k_iA_t(x)\}L_t(x) \\ A_{t+1}(x) &= \int_0^M \frac{1}{C} \exp\{-D_{AP}((1 - \mu_L) \exp\{-k_iA_t(x)\}L_t(x))\} \\ &\quad \times [P_t(y) + (1 - \mu_A)A_t(y)] dy. \end{aligned} \tag{10}$$

In cultures of *T. brevicornis*, animals can occupy space right up to the boundary, but cannot pass through the boundary walls. We note this model preserves such no-flux boundary conditions at both endpoints. That is, if  $\frac{\partial}{\partial x}\vec{n}_0|_{x=0,\pi} = 0$ , then  $\frac{\partial}{\partial x}\vec{n}_t|_{x=0,\pi} = 0$  for all  $t > 0$ .

### 5 Model Simulation Results

To simulate this model, we must first choose initial conditions. We note that an initial condition with a uniform spatial distribution will remain a uniform spatial distribu-

**Fig. 5** Equilibrium attractor of spatial SLPA model. Attractor is spatially uniform with  $(S_e, L_e, P_e, A_e) = (12.21, 71.77, 2.59, 163.8)$ . Parameter values used for SLPA model are maximum likelihood estimates:  $b = 11.41$ ,  $\mu_L = 0.134$ ,  $\mu_A = 0.0158$ ,  $c_{es} = 0.0135$ ,  $c_{ea} = 0.0223$ ,  $c_{el} = 0.0169$ ,  $k_i = 0.0194$ .  $D_{AP} = 1$ ,  $D_{LA} = 0.05$ , and  $M = 1$ . Initial condition:  $L_0 = 100$ ,  $A_0 = 0$  on the subinterval of domain  $[0, 0.25]$



tion for all time since no preferences for different spatial locations are built into the model. Rather, the fraction of individuals leaving or settling at a given location depends only on the population density at that location. There are many non-uniform initial distributions one could consider. We restrict our investigation to initial conditions  $(0, L_0(x), 0, A_0(x))$ . We can think of this initial condition as representing a biological invasion of a new environment; the only possible invaders are the dispersing stages,  $L$  and  $A$ .

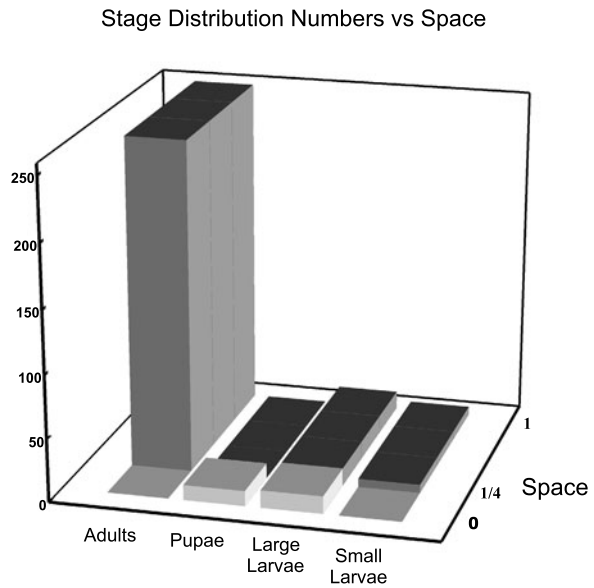
We subject our initial vector  $(0, L_0(x), 0, A_0(x))$  to a uniform distribution on a subinterval of the spatial domain  $[0, m]$ . Thus  $L_0(x) = C_L$ ,  $A_0(x) = C_A$  for  $0 \leq x \leq m < M$  and  $L_0(x) = 0, A_0(x) = 0$  for  $m < x \leq M$ . These initial conditions can be easily reproduced experimentally.

Extensive numerical simulations show that for this set of initial conditions, under the maximum likelihood SLPA model parameter estimates in Table 1, the spatial SLPA model admits multiple attractors. These attractors include a spatially uniform distribution and a “patchy” distribution.

The patchy attractor consists of a spatially uniform equilibrium  $(S_e, L_e, P_e, A_e)$  on  $[0, m]$  and a spatially uniform equilibrium  $(S_e^*, L_e^*, P_e^*, A_e^*)$  on  $(m, M]$ . For  $D_{AP}$  large enough, adults are essentially restricted to either  $[0, m]$  or  $(m, M]$  with increased densities of pupae in the other patch. Thus, the model predicts that pupae form a “nest,” i.e., a patch of pupae not occupied by adults. As we will see in Sect. 6, these nests have been observed in experimental cultures of *T. brevicornis*.

These findings are illustrated in Figs. 5 and 6, which show the uniform and patch attractors resulting from the same set of parameter values (SLPA model parameters from Table 1,  $D_{AP} = 1, D_{LA} = 0.05$ ) but different initial conditions. Note that the domain size  $M$  does not affect model attractors. For simulations in this paper, we used  $M = 1$  and  $m = 0.25$ . In Fig. 5, the initial conditions are  $L_0(x) = 100, A_0(x) = 0$  for  $x \in [0, 0.25]$  and the attractor is a spatially uniform equilibrium with

**Fig. 6** Equilibrium attractor of spatial SLPA model, consisting of two patches with  $(S_e, L_e, P_e, A_e) = (0.015, 13.93, 12.06, 0.0016)$  on  $[0, 0.25]$  and  $(S_e^*, L_e^*, P_e^*, A_e^*) = (6.58, 13.92, 0.08, 259.4)$  on  $(0.25, 1]$ . Parameter values used for SLPA model are the maximum likelihood estimates:  $b = 11.41, \mu_L = 0.134, \mu_A = 0.0158, c_{es} = 0.0135, c_{ea} = 0.0223, c_{el} = 0.0169, k_i = 0.0194, D_{AP} = 1, D_{LA} = 0.05, m = 0.25,$  and  $M = 1$ . Initial condition:  $A_0 = 100, L_0 = 0$  on the subinterval of domain  $[0, 0.25]$



$(S_e, L_e, P_e, A_e) = (12.21, 71.77, 2.59, 163.8)$ . In Fig. 6, the initial conditions are  $L_0(x) = 0, A_0(x) = 100$  for  $x \in [0, 0.25]$ , and the result is a two patch spatial distribution that equilibrates in time. The population density on the left patch  $[0, 0.25]$  is  $(S_e, L_e, P_e, A_e) = (0.015, 13.92, 12.06, 0.0016)$  and the population density on the right patch  $(0.25, 1]$  is  $(S_e^*, L_e^*, P_e^*, A_e^*) = (6.58, 13.92, 0.08, 259.4)$ .

The two attractors in Figs. 5 and 6 are not the only possible attractors for this set of parameter values, but they are the most common for the set of initial conditions we investigated (a uniform distribution of dispersing stages on a subinterval of the domain) and they are also the two attractors seen in the laboratory, as described in Sect. 6. The initial condition  $L_0(x) = 0, A_0(x) = 25$  for  $x \in [0, 0.25]$  (see Fig. 7) results in a third type of attractor, a nonequilibrium “recurrent nest” characterized by time intervals where one patch has increased densities of pupae and essentially no adults present.

All initial conditions of the form  $(0, C_L, 0, 0), x \in [0, m]$  converge to the spatially uniform attractor. Initial conditions of the form  $(0, 0, 0, C_A), x \in [0, m]$  may result in the patch attractor, the spatially uniform attractor, or another attractor (such as the recurrent nest) depending on the value of  $C_A$  and  $m$ . Basins of attraction are shown in Fig. 8.

When inhibition is absent ( $k_i = 0$ ) the patchy distribution was not found after extensive numerical simulation. The only attractor observed was the spatially uniform distribution, suggesting that inhibition is an important factor for the segregation of life cycle stages in a homogeneous habitat.

The initial condition of  $L_0(x) = 0, A_0(x) = 100$  on the left quarter of the domain ( $x \in [0, 0.25]$ ) leads to a patchy attractor for many values of the inhibition coefficient  $k_i$ , including  $0.01 \leq k_i \leq 0.1$ . For these same values of  $k_i$ , an initial condition of  $L_0(x) = 100, A_0(x) = 0$  for  $x \in [0, 0.25]$  leads to a spatially uniform attractor.

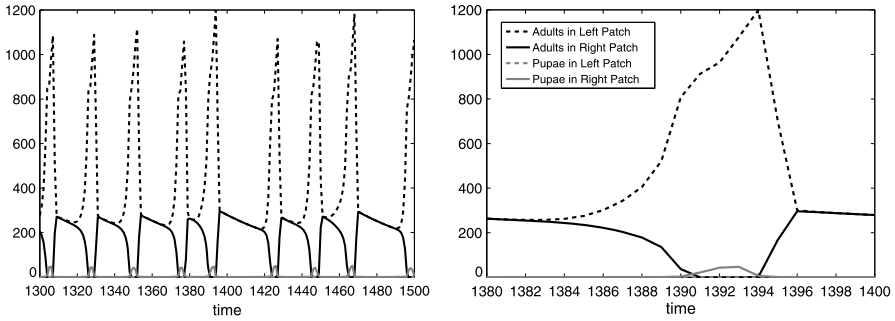


**Fig. 7** Recurrent nest attractor of spatial SLPA model, characterized by periods of low adult density and high pupal density in one patch. The left patch is the interval  $[0, 0.25]$  and the right patch is the interval  $(0.25, 1]$ . Parameter values used for SLPA model are the maximum likelihood estimates:  $b = 11.41, \mu_L = 0.134, \mu_A = 0.0158, c_{es} = 0.0135, c_{ea} = 0.0223, c_{el} = 0.0169, k_i = 0.0194, D_{AP} = 1, D_{LA} = 0.05, m = 0.25$  and  $M = 1$ . Initial condition:  $A_0 = 25, L_0 = 0$  on the subinterval of domain  $[0, 0.25]$

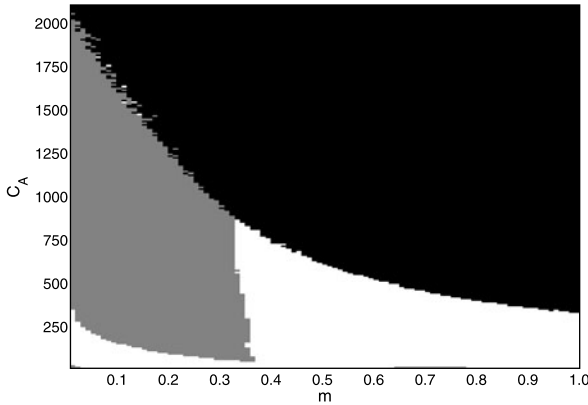


**Fig. 8** Basins of attraction for spatial SLPA model with initial conditions of the form  $(0, 0, 0, C_A)$  on the subinterval of the domain  $[0, m]$ . Model (10) was simulated for values of  $C_A$  between 0 and 2100 in increments of 10, and values of  $m$  between 0 and 1 in increments of 0.01. Initial conditions converging to the patchy attractor are shown in gray, those converging to the spatially uniform attractor are shown in black, and initial conditions resulting in other attractors, such as the recurrent nest, are left white. Model parameters:  $b = 11.41, \mu_L = 0.134, \mu_A = 0.0158, c_{es} = 0.0135, c_{ea} = 0.0223, c_{el} = 0.0169, k_i = 0.0194, D_{AP} = 1$  and  $D_{LA} = 0.05, M = 1$ . An increase in  $D_{AP}$  to  $D_{AP} = 2$  extends the basin of attraction of the patchy attractor to the right, while an increase in  $D_{LA}$  to  $D_{LA} = 0.5$  lowers the boundary marking the transition to the spatially uniform attractor. When  $k_i = 0$ , all initial conditions shown here converge to the spatially uniform attractor

Figure 9 shows how the spatially uniform and patchy attractors change as inhibition increases. While the patchy attractor remains almost constant as  $k_i$  increases, the spatially uniform attractor is more sensitive to the degree of inhibition. As  $k_i$  increases, the densities of small and large larvae increase while the densities of pupae and adults decrease.

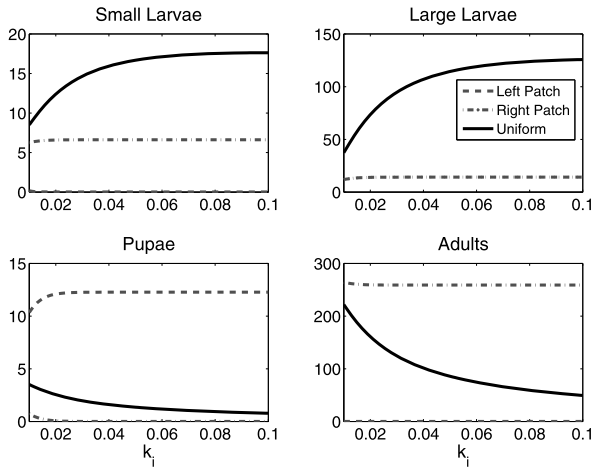


**Fig. 9** Comparison of equilibrium stage densities for patchy and uniform attractors as a function of inhibition,  $k_i$ , on the spatial domain  $[0, 1]$ . *Black curves* represent the equilibrium density of the spatially uniform attractor. Simulations were started with an initial distribution of  $L_0(x) = 100$ ,  $A_0(x) = 0$  on  $[0, 0.25]$ . The *grey curves* represent the equilibrium densities of the patchy attractor; the *dashed line* gives the density in the left patch ( $0 \leq x \leq 0.25$ ) and the *dot-dashed line* gives the density in the right patch. Simulations were started with an initial distribution of  $L_0(x) = 0$ ,  $A_0(x) = 100$  on  $[0, 0.25]$ . All other parameter values used (for all simulations) were:  $b = 11.41$ ,  $\mu_L = 0.134$ ,  $\mu_A = 0.0158$ ,  $c_{es} = 0.0135$ ,  $c_{ea} = 0.0223$ ,  $c_{el} = 0.0169$ ,  $D_{AP} = 1$ , and  $D_{LA} = 0.05$

We can also compare the total population size, as well as the number of individuals in each stage, for the two attractors. Figure 10 shows that as the degree of inhibition  $k_i$  increases (i.e. it takes fewer adults to inhibit the same fraction of large larvae) the total population size decreases for both attractors. Yet the *difference* in total population size between the attractors also decreases and for  $k_i$  large enough the total population size is greater for the patchy distribution than the uniform distribution. The relative density of each of the classes also changes as the degree of inhibition increases. For  $k_i = 0.01$ , we see from Fig. 10 that the uniform attractor has a larger total density of all stages compared to the patchy attractor. For  $k_i = 0.0194$  (the maximum likelihood parameter estimate for historical *T. brevicornis* census data), the patchy attractor has a greater number of pupae and adults.

## 6 Comparison of Model Predictions and Experimental Observations

Patterns similar to those in Fig. 1 are seen in a box similar in size but that can be subdivided into smaller rectangles by inserting removable panels. Figure 11 shows three replicate cultures in habitats two-thirds the length as those in Fig. 1 but only a quarter of the width. In each replicate on the left side of the figure, there is a region of high pupal density that we refer to as a “pupal nest.” The pupal nest persists over time; new callow (light brown) adults seen emerging from the pupal nest indicates large larvae return there to pupate. Pupal nests have also been observed in domains longer than those shown in Fig. 11, but the pupal nest is not the only pattern observed

**Fig. 10** Comparison of population sizes for patchy and uniform attractors as a function of inhibition,  $k_i$ , on the spatial domain  $[0, 1]$ . Solid and dashed curves represent the total number of individuals in each stage, as well as the total population size, for the spatially uniform and patchy attractors, respectively. For each value of  $k_i$ , the total number of small larvae, large larvae, pupae, adults, and total population size (the sum of all stages) are calculated for each attractor by integrating each equilibrium distribution (given in Fig. 9) from 0 to 1 with respect to the spatial variable  $x$

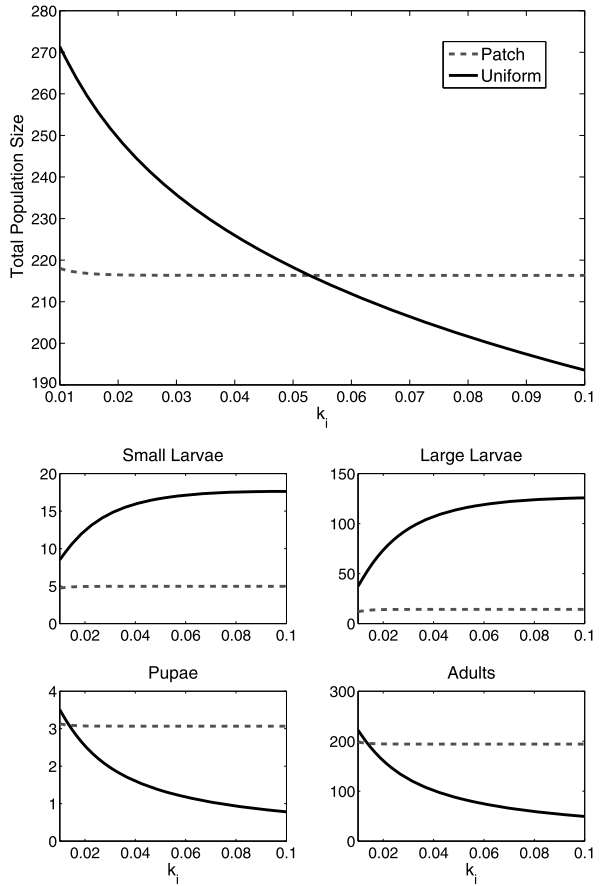


**Fig. 11** Culture of *Tribolium brevicornis*. Three replicates show segregation of adults and pupae, illustrating the pupal nest on the left side of each row. Each row was started with large larvae and adults on the left half of the domain. They were contained in this subhabitat for 6 weeks, then a panel was removed and they were allowed to disperse throughout the entire row. Photo was taken a week after the door was opened

**Fig. 12** Culture of *Tribolium brevicornis*. Panels are removed at ends of rows to allow animals to move throughout the entire domain. The culture was started with adults in the upper right corner, and the beetles were immediately permitted to disperse. No pupal nest is established



in cultures with this type of domain. Rather, the pattern formed depends on the initial condition of the culture and whether the pupal nest has had a chance to establish itself before widespread dispersal takes place. Figure 12 shows a culture of *T. brevicornis* in which a pupal nest was never established and exhibits no segregation of life cycle stages. We note that the domain in Fig. 12 is longer than those in Fig. 11 but is the same width.

The culture in Fig. 12 was started with *T. brevicornis* adults in the upper right corner of the box. The adults immediately spread out and no pupal nest was ever established. To simulate this situation where adults are immediately allowed to disperse, the spatial SLPA model needs to be started with an initial condition of only *L* stage individuals. Since reproduction occurs before dispersal in the model, *L* stage individuals will all pupate immediately (since no *A* stage individuals are present to delay pupation) and emerge as adults. These adults will then disperse according to (6), the adult dispersal kernel. The absence of pupae results in the adults dispersing uniformly throughout the entire domain, matching what is seen experimentally. Therefore, a laboratory initial condition of only adults who are immediately permitted to disperse corresponds to a model simulation initial condition of only large larvae. In two time steps, this initial condition will result in a cohort of dispersing adults, with no other stages present.

The three cultures in Fig. 11 were started with *L* and *A* stage animals mixed together on the left half of the domain. The movement of these animals was restricted by a panel inserted to divide each row of flour in half. After 6 weeks, the panel was removed and animals were able to migrate into the right half of each row. This resulted in the formation of a pupal nest. Such a patchy attractor can be predicted by the model for initial conditions of adults only, or of both adults and large larvae. Since reproduction occurs before dispersal in the model, the initial condition of *A* only results in *A* and *S* stage individuals present at the time of dispersal. The small larvae do not disperse, but the *A* spread out across the entire domain. The next time step, small larvae become large larvae. These large larvae will not disperse provided the adult density is low enough (this depends on the decision parameter  $D_{LA}$ ) from the adults spreading out over the entire habitat. At the next time step, these same large larvae will pupate in their original location if adult density is low enough (this depends on the inhibition parameter  $k_i$ ). Once they do, a pupal nest has been established and it will be avoided by the adults in subsequent time steps.

If the model is instead started with both  $L$  and  $A$  stage individuals present, a situation similar to the one just described (for an initial condition of  $A$  only) occurs. The initial density of  $A$  may be great enough to inhibit large larvae. If so, a fraction of them, determined by  $\gamma_L$ , will disperse uniformly over the whole domain along with the adults. The next time step, adults should be spread out enough to allow all large larvae to pupate. Unless all  $L$  dispersed, the density of  $L$  should be greater in their starting interval than the rest of the domain and this will result in a greater density of pupae and mark the location of the pupal nest. The moment the door is opened in the laboratory culture corresponds to halfway through a model time step—after reproduction but right before dispersal.

Over time, the nest persists both in model simulations (since the patchy attractor is an equilibrium attractor) and laboratory cultures, in the location it was originally established. This location does not have to be at the edge of the domain; it can be an interval in the center of the domain as well. Adults can become very dense outside of the nest, and this may provide a barrier to any invading species, including those where adults cannibalize pupae.

In summary, the spatial SLPA model (10) has been able to predict observed spatial segregation in *T. brevicornis*. We were able to further connect model (10) with experimental observations for select cases, providing experimental support for the multiple spatial attractors predicted by the spatial SLPA model. The fact that we were unable to find initial conditions leading to the patchy attractor when the inhibition parameter  $k_i = 0$  suggests that the inhibition of large larvae is a necessary condition for spatial segregation of life cycle stages. This is consistent with the absence of surface patterns in non-inhibiting species such as *T. castaneum* and *T. confusum*. Furthermore, the model predicts that for a species with the parameterized inhibition level of *T. brevicornis* ( $k_i = 0.0194$ ), the spatial separation of life cycle stages can affect the relative total population sizes of the stages. Specifically, the total number of pupae and adults are higher for the patchy attractor relative to the uniform attractor. Sexually mature adults become the dominant stage in the patchy attractor, whereas the immature large larvae dominate for the spatially uniform attractor.

## 7 Discussion

The patterns observed in *T. brevicornis* are striking and unique, with adults clearly aggregating together in cultures of many different sizes and shapes. To the authors' knowledge, such patterns have not been documented for any other *Tribolium* species, even other inhibiting species such as *T. freemani*. However, *T. freemani* larvae are inhibited by other larvae, so escaping high densities of adults would not help them pupate. In fact, laboratory cultures of this species almost always result in a strong larval bottleneck with very few adults present. In *T. brevicornis*, on the other hand, when larvae escape to areas of low adult density they may immediately pupate (provided they are old enough). Mathematically, inhibition plays an important role in the formation of spatial segregation. The number of initial conditions giving rise to the patchy attractor of the spatial SLPA model decreases as the severity of inhibition decreases; the patchy attractor could not be found when the inhibition parameter  $k_i$  was set to zero.

Density dependent dispersal can have a notable affect on population size and structure of the equilibrium stage-class vector for inhibiting species. All other parameters equal, the model always predicts a non-inhibitor will have greater total population sizes than an inhibiting species. This makes sense intuitively, since 100% of larva surviving mortality go on to pupate in the absence of inhibition. Inhibition only decreases this number and can only decrease total population size.

We also compared population numbers for an inhibiting species in two different spatial structures, finding that if inhibition is strong enough, the spatially segregated model attractor has a greater population size than the spatially uniform attractor. This also makes biological sense. If a species is a strong inhibitor, very few larvae will be able to pupate once an adult cohort has been established. Eggs will still be laid but few new sexually mature adults will be produced. The model shows that separating the stages spatially and giving the larvae a refuge in which to pupate results in higher population numbers.

For the parameterized inhibition level of *T. brevicornis*, spatial segregation does not result in greater total population numbers, but it does shift the composition of the equilibrium stage vector ( $S^*$ ,  $L^*$ ,  $P^*$ ,  $A^*$ ) in favor of higher numbers of  $P^*$  and  $A^*$ . If dispersal is really important in this species' natural habitat, adults may be the primary invaders of new colonies. Increasing the number of adults could mean larger founding populations at their next location.

As noted above, the spatial SLPA model exhibits multiple attractors, including a spatially uniform attractor and a patchy attractor with pupae and adults spatially separated. These two attractors have been seen in experimental cultures of *T. brevicornis*. The spatial segregation of adults and other life cycle stages has been observed in many different sizes and shapes of *T. brevicornis* cultures. However, the shape of the surface of the container used in Figs. 11 and 12 are the closest to being one-dimensional and also produces the most reproducible patterns. Vertical cross sections through each row yield an approximately uniform distribution of beetles and so the pattern can be collapsed to one dimension more easily than that in Fig. 1.

Figure 11 clearly shows the formation of the pupal nest that is predicted by the patchy attractor of the spatial SLPA model, while Fig. 12 shows the uniform attractor of the spatial SLPA model. As discussed in Sect. 6, initial conditions for the laboratory cultures are consistent with those used in model simulations. A patchy attractor is reached if a pupal nest has a chance to be established. If a culture is started with adults who immediately have the opportunity to disperse, they spread out, taking advantage of the entire habitat. If a culture is started with large larvae and adults who are contained in a subsection of the habitat, the adults inhibit the large larvae and prevent them from pupating. Once the "door" is opened, allowing them to access to the entire habitat, the adults disperse quickly. The large larvae do not get very far before sensing conditions are right to pupate, and a pupal nest is established. Once the nest is established, it persists over time. New adults emerge and leave the nest, while large larvae from outside the nest have been observed returning to the nest.

Our results may have important implications for future multispecies competition studies. Many experiments have been done on the subject of competition between closely related species (Leslie et al. 1968). In cultures of *T. confusum* and *T. castaneum*, almost all cultures saw one species exclude the other according to the principle

of competitive exclusion. The winning species depended on initial conditions. The LPA model has had previous success modeling competition; an extension of the LPA model to a competition model has led to potential counterexamples to the principle of competitive exclusion, explaining prolonged coexistence between two species of closely related flour beetles observed by Park (Edmunds et al. 2003).

Jillson and Costantino experimented with competition between *T. brevicornis* and *T. castaneum*. Every culture resulted in competitive exclusion, with *T. brevicornis* always being eliminated regardless of initial conditions (Jillson and Costantino 1980; Costantino and Desharnais 1991). Inhibition of *T. brevicornis* larvae is not species specific, so contact with *T. castaneum* adults will also delay pupal metamorphosis (Jillson and Costantino 1980). Furthermore, *T. castaneum* adults will cannibalize *T. brevicornis* pupae in addition to their own. Thus, *T. brevicornis* has a two-fold disadvantage. Their larvae are inhibited by both species' adults and their larvae that do manage to pupate are now subject to cannibalism.

We note that while the environment is uniform at the onset of the culture seen in Fig. 11, it does not remain so. *T. brevicornis* deliberately modifies the habitat of the nest; it becomes devoid of any nutritious value, possessing only metabolic wastes and quinones that are secreted through the odoriferous glands. The altered section of the habitat seemingly becomes a refugium for larvae to undergo pupation. The high densities of *T. brevicornis* adults surrounding the nest may also provide a barrier to potentially cannibalistic invaders.

These factors suggest spatial structure may play an important role when considering competition between *T. brevicornis* and a non-inhibiting species such as *T. castaneum* or *T. confusum*. If *T. brevicornis* has a chance to establish a pupal nest, the species may be better able to survive an invasion by another species of the genus *Tribolium*.

**Acknowledgements** This work was done as part of S.L. Robertson's Ph.D. thesis, Spatial patterns in stage-structured populations with density dependent dispersal, Interdisciplinary Program in Applied Mathematics, University of Arizona, 2009, and was supported in part by National Science Foundation grants DMS-0414212 and DMS-0443803.

## References

- Benoit, H. P., et al. (1998). Testing the demographic consequences of cannibalism in *Tribolium confusum*. *Ecology*, 78, 2839–2851.
- Costantino, R. F., & Desharnais, R. A. (1991). *Population dynamics and the Tribolium model: genetics and demography*. New York: Springer.
- Cushing, J. M. (2004). The LPA model. *Fields Inst. Commun.*, 42, 29–55.
- Cushing, J. M., et al. (2003). *Chaos in Ecology: Experimental Nonlinear Dynamics*, vol. 1. *Theoretical Ecology Series*. New York: Academic Press.
- Dennis, B., et al. (1995). Nonlinear demographic dynamics: Mathematical models, statistical methods, and biological experiments. *Ecol. Monogr.*, 65, 261–281.
- Edmunds, J., et al. (2003). Park's *Tribolium* competition experiments: a non-equilibrium species coexistence hypothesis. *J. Anim. Ecol.*, 72, 703–712.
- Ghent, A. W. (1966). Studies of behavior of the *Tribolium* flour beetles. II. Distributions in depth of *T. castaneum* and *T. confusum* in fractionable shell vials. *Ecology*, 47, 355–367.
- Harrison, R. G. (1980). Dispersal polymorphisms in insects. *Ann. Rev. Ecol. Syst.*, 11, 95–118.
- Hastings, A., & Costantino, R. F. (1991). Oscillations in population numbers: age-dependent cannibalism. *J. Anim. Ecol.*, 60, 471–482.

- Hill, C. (1988). Life cycle and spatial distribution of the amphipod *Pallasea quadrispinosa* in a lake in northern Sweden. *Holarctic Ecology*, *11*, 298–304.
- Hunte, W., & Myers, R. A. (1984). Phototaxis and cannibalism in gammaridean amphipods. *Mar. Biol.*, *81*, 75–79.
- Jillson, D. A., & Costantino, R. F. (1980). Growth, distribution, and competition of *Tribolium castaneum* and *Tribolium brevicornis* in fine-grained habitats. *Am. Nat.*, *116*, 206–219.
- Jormalainen, V., & Shuster, S. M. (1997). Microhabitat segregation and cannibalism in an endangered freshwater isopod, *Thermosphaeroma thermophilum*. *Oecologia*, *111*, 271–279.
- Kisimoto, R. (1956). Effect of crowding during the larval period on the determination of the wing form of an adult plant-hopper. *Nature*, *178*, 641–642.
- Leonardsson, K. (1991). Effects of cannibalism and alternative prey on population dynamics of *Saduria entomon* (Isopoda). *Ecology*, *72*, 1273–1285.
- Leslie, P. H., Park, T., & Mertz, D. B. (1968). The effect of varying the initial numbers on the outcome of competition between two *Tribolium* species. *J. Anim. Ecol.*, *37*, 9–23.
- Ribes, M., et al. (1996). Small scale spatial heterogeneity and seasonal variation in a population of a cave-dwelling Mediterranean mysid. *J. Plankton Res.*, *18*, 659–671.
- Robertson, S. L. (2009) Spatial patterns in stage-structured populations with density dependent dispersal, PhD Thesis, University of Arizona.
- Robertson, S. L., & Cushing, J. M. (2011a). Spatial segregation in stage-structured populations with an application to *Tribolium*. *Journal of Biological Dynamics*, *5*(5), 398–409.
- Robertson, S. L., & Cushing, J. M. (2011b). A bifurcation analysis of stage-structured density dependent integrodifference equations. *J. Math. Anal. Appl.* doi:[10.1016/j.jmaa.2011.09.064](https://doi.org/10.1016/j.jmaa.2011.09.064).
- Sokoloff, A., et al. (1980). Observations on populations of *Tribolium brevicornis* (Le conte) (Coleoptera, Tenebrionidae). I. Laboratory observations of domesticated strains. *Res. Popul. Ecol.*, *22*, 1–12.